2021 43rd Annual International Conference of the
IEEE Engineering in Medicine & Biology Society (EMBC)
Oct 31 - Nov 4, 2021. Virtual Conference

Cuff-Less Blood Pressure Estimation via Small Convolutional Neural Networks

Weinan Wang*, Pedram Mohseni†, Kevin Kilgore+ and Laleh Najafizadeh*

Abstract— **Deep learning-based cuff-less blood pressure (BP) estimation methods have recently gained increased attention as they can provide accurate BP estimation with only one physiological signal as input. In this paper, we present a simple and effective method for cuff-less BP estimation by training a small-scale convolutional neural network (CNN), modified from LeNet-5, with images created from short segments of the photoplethysmogram (PPG) signal via visibility graph (VG). Results show that the trained modified LeNet-5 model achieves an error performance of 0.184 ± 7.457 mmHg for the systolic BP (SBP), and 0.343 ± 4.065 mmHg for the diastolic BP (DBP) in terms of the mean error (ME) and the standard deviation (SD) of error between the estimated and reference BP. Both the SBP and the DBP accuracy rank grade A under the British Hypertension Society (BHS) protocol, demonstrating that our proposed method is an accurate way for cuff-less BP estimation.**

I. Introduction

Continuous and non-invasive blood pressure (BP) monitoring techniques are highly desirable for managing hypertension and preventing the progression of cardiovascular diseases. Existing brachial cuff-based BP monitors are not capable of continuous monitoring of the BP levels due to their requirement of intermittent manual operation, and the needed prolonged $30 \sim 40$ seconds interval for obtaining one pair of systolic BP (SBP) and diastolic BP (DBP) readings. Therefore, cuff-less BP monitoring methods have been pursued in the past decades.

Existing cuff-less BP estimation methods generally fall into two categories: model-driven and data-driven. Model-driven approaches aim at deriving theoretical models that estimate BP from pulse transit time (PTT), based on the relationship between the BP and the pulse wave velocity (PWV). These methods usually require to receive input from at least two physiological signals (placed at proximal and distal spots). On the other hand, data-driven methods enable obtaining estimates of BP from only one physiological signal (e.g. photoplethysmogram (PPG)) [1], [2].

Recently, deep learning models have been applied to enable end-to-end learning from raw PPG signals to BP estimation. The strong feature-learning capability of deep neural networks (DNNs) enables embedded feature extraction from raw or simply-transformed PPG signals, eliminating the procedures of manually selecting and extracting features. For example, in [3], a customized spectral-temporal DNN architecture was used by combining multiple residual networks (ResNets) and gated recurrent units (GRUs) to estimate BP from raw PPG signals, and mean absolute errors (MAE) of 9.43 mmHg and 6.88 mmHg were reported for SBP and DBP, respectively. In another example, in [4] a siamese convolutional neural network (CNN) inspired by AlexNet [5] was used to learn from the spectrogram of 30-second PPG windows, where results of 7.34 (MAE) and 8.65 (standard deviation of error (SD)) mmHg for SBP, and 3.91 (MAE) and 4.48 (SD) mmHg for DBP were obtained. However, these works use complicated, non-ordinary DNN architectures, making the implementation of these algorithms difficult.

Inspired by recent efforts of applying image classification network architectures to images created from sensor signals [6], [7], [8], [9], in this work, we propose a cuff-less BP-estimation method in which images of short segments of PPG signals are created by visibility graph (VG). In contrast to our previous work [9], where transfer learning was used, here, we use a modified LeNet-5 CNN, which is simple and easily implementable and achieves much better performance. Additionally, we compare the performance of our LeNet-5 CNN model with three other DNN architectures. As it will be shown, our accuracy results for both the SBP and the DBP rank grade A under the British Hypertension Society (BHS) protocol, demonstrating that our proposed method is an accurate and easy way for cuff-less BP estimation.

The rest of this paper is organized as follows. The proposed method is introduced in Section II. The BP estimation results are presented and discussed in Section III, and the paper is concluded in Section IV.

II. Methods

A. Dataset Information and Pre-processing

The "Cuff-Less Blood Pressure Estimation Dataset" from the University of California Irvine (UCI) Machine Learning Repository [10], which is a subset of the Multi-parameter Intelligent Monitoring in Intensive Care (MIMIC) II waveform database [11], was used in this study. Recorded directly from the intensive care unit (ICU), a large portion of the MIMIC database contains contaminated and unreliable signals, while in the UCI dataset, high-quality records from the MIMIC

This work was supported by Craig H. Neilsen Foundation Award # 598202.

* Department of Electrical and Computer Engineering, Rutgers University, Piscataway, NJ 08854, USA. {ww329, laleh.najafizadeh}@rutgers.edu.

† Department of Electrical, Computer, and Systems Engineering, Case Western Reserve University, Cleveland, OH, USA. pxm89@case.edu.

+ Departments of Orthopaedics and Physical Medicine & Rehabilitation, Case Western Reserve University and MetroHealth System, Cleveland, OH, USA. klk4@case.edu.

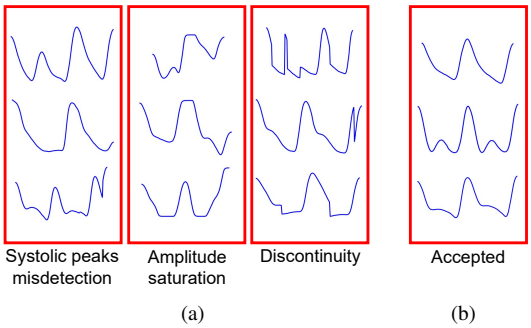

Fig. 1. (a) Examples of PPG windows with defects that were removed from the dataset. (b) Examples of accepted PPG windows.

database have been included. The UCI dataset contains synchronized PPG, electrocardiogram (ECG), and arterial blood pressure (ABP) signals sampled at 125 Hz. In this study, only the PPG and the ABP signals were used.

12000 records of the UCI dataset were downloaded from [12], and 200 records of PPG and ABP signals with duration longer than 500 seconds were used. The reference SBP and DBP values were extracted from the ABP signals, and were used as ground-truth labels for model training and testing.

Records of PPG signals were separated into non-overlapping beat-to-beat windows, such that one pair of SBP/DBP estimation could be made from each window. Each window was located by 3 consecutive systolic peaks and contained 1 complete PPG cycle. To locate the position of the systolic peaks, the algorithm in [13] was used. A total number of 37228 PPG windows were obtained from the 200 selected records. Reference BP values of these PPG windows were extracted from their corresponding ABP signal.

After the extraction of PPG windows, a manual selection process was employed to exclude windows having any of the following defects:

- *Missing systolic peaks*: Due to the variations in the morphology of PPG waveforms, misdetection of the systolic peaks could occur. Windows containing non-systolic peaks or more than 3 systolic peaks were excluded.
- *Amplitude saturation*: In some of the extracted PPG windows, the waveform had saturated amplitudes (e.g. flat horizontal lines), which could have been caused by improper placement of the sensor during the recording. Therefore, these windows were removed.
- *Discontinuity*: The UCI dataset is created by concatenating high-quality signal blocks from the MIMIC database [10]. If a window is located across the intersection of two blocks, then the PPG waveform in the window will have discontinuities. These windows that do not represent realistic PPG recordings were excluded.
- *Overlength*: In general, it is expected that the human heart rate is above 60 beats per minutes (1 Hz). Therefore, a proper PPG window located by 3 consecutive systolic peaks should contain no more than 250 samples. Windows with duration longer than this length were removed.

Fig. 1(a) shows some examples of the PPG windows with misdetection, saturation and discontinuity defects, while Fig. 1(b) displays examples of accepted PPG windows. After this selection process, 3% of PPG windows were removed from the dataset, and 36117 PPG windows from 169 records were accepted. The mean and standard deviation of the reference SBP and DBP values in the accepted dataset were 136.95 ± 22.43 mmHg and 63.97 ± 9.73 mmHg, respectively, indicating sufficient BP variation for training and testing the model.

B. Image Creation

The process of creating images from PPG recordings was explained in [9]. Briefly, VG is a graph creation method that transforms time series into undirected graphs [14], [15], and have been previously used in processing of physiological signals [16], [17]. To construct the VG for a time series, each sample in the time series is considered as a node. The graph is then formed by considering the *natural visibility* between every two nodes. As such, the VG preserves the morphological features of the time series. Following this process, for each of the PPG windows zero-mapped to 250 samples, the VG is formed. Then, the adjacency matrix for each graph is mapped into a single-channel 250×250 gray-scale image, capturing the temporal-domain features of the PPG waveform [18]. These VG images were then consequently used to train DNNs for BP estimation.

C. Architectures of DNNs

Fig. 2 displays the architecture of four DNNs experimented in this study. These architectures belong to the following categories.

1) Modified LeNet-5: LeNet-5 [19] is a classic CNN architecture taking single-channel 32×32 image as input for hand-written digit classification. While the original LeNet-5 architecture uses hyperbolic tangent activation function and average pooling, in this work, they were replaced with a more modern combination of ReLU activation and max pooling. The size, amount and activation functions of the dense layers were also modified in accordance with the 250×250 VG inputs and 2 numerical outputs of SBP and DBP.

2) Modified electroencephalogram (EEG) classification network: For performance comparison, the EEG classification network used in [8] was also experimented in this study. [8] shares a similar idea with our work as it utilizes Gramian Angular Summation Field (GASF) to create images from EEG signals to detect epilepsy. While the LeNet architecture utilizes pooling after each convolutional layer, the EEG classification network uses larger filter stride to downsample the feature map, and includes an additional batch normalization layer.

The original network proposed in [8] used 3×3 convolution kernel. In this study, an additional architecture using the same 5×5 kernel as LeNet was also included for comparison. For both the 3×3 kernel and the 5×5 kernel settings, the dense layers after the convolutional layers were modified for regression instead of classification, keeping a consistent layout with the modified LeNet-5.

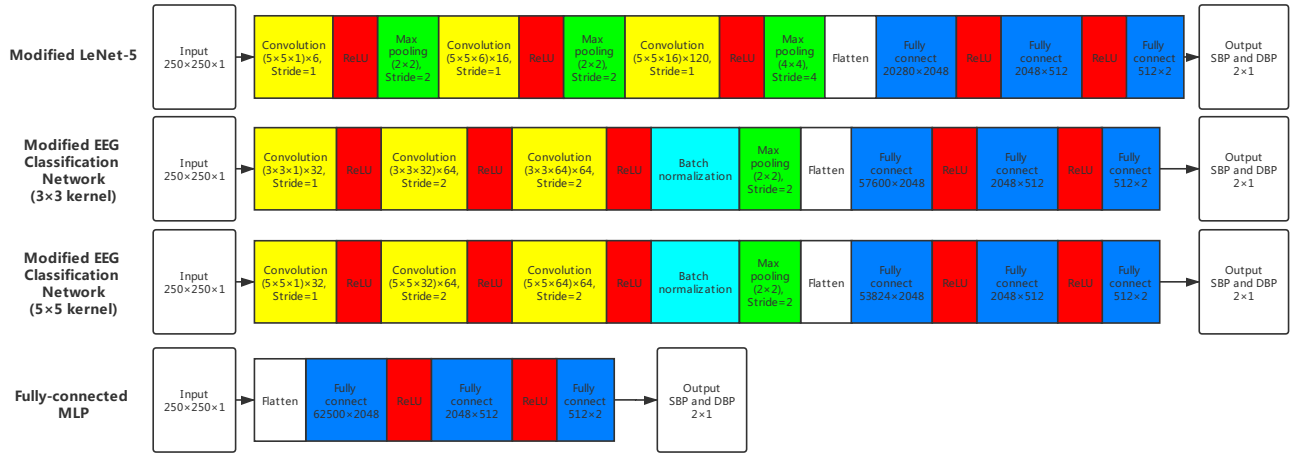

Fig. 2. The architecture of four DNN models experimented in this study. Layers of the same type are shown with the same color.

TABLE I

SUMMARY OF REGRESSION RESULTS USING FOUR DIFFERENT DNN ARCHITECTURES.

Model Type	**BP Estimation Accuracy on Testing Set (N=5417)**					
	SBP			**DBP**		
	R	**ME±SD (mmHg)**	**RMSE (mmHg)**	**R**	**ME±SD (mmHg)**	**RMSE (mmHg)**
Modified LeNet-5	0.944	0.184±7.457	7.458	0.906	0.343±4.065	4.079
Modified EEG CNN, 5×5 kernel	0.940	0.173±7.709	7.711	0.889	0.144±4.409	4.412
Modified EEG CNN, 3×3 kernel	0.924	0.058±8.608	8.608	0.878	0.124±4.599	4.601
Fully connected MLP	0.923	-0.510±8.695	8.710	0.869	0.237±4.777	4.783

3) Fully-connected multi-layer perceptron (MLP): We also tested the performance of MLP on the BP estimation task, which is simply the dense layers after the convolutional layers of the CNNs described above, taking the flattened VG images directly as input. The idea is to use the performance of MLP as a baseline reference to see how well the convolutional filters in the previous 3 CNN settings were extracting features from VG images.

III. RESULTS AND DISCUSSIONS

For each of the four DNN architectures, 70%, 15% and 15% of the data were used for training, validating and testing, respectively. The regression performance of each model is summarized in Table I. The best BP estimation accuracy comes from the modified LeNet-5 model, with an error performance of 0.184 ± 7.457 mmHg for SBP, and 0.343 ± 4.065 mmHg for DBP. In terms of error deviation and RMSE, the modified EEG classification network with 5×5 kernel has close but inferior accuracy compared to the modified LeNet-5. Meanwhile, the EEG network with 3×3 kernel achieves a similar accuracy with the MLP, both being much inferior to the two CNNs with 5×5 kernel, which indicates a clear advantage of using 5×5 kernel for extracting features from VG.

Under the optimal setting using the modified LeNet-5 model, our SBP and DBP performances are within the limits of the American National Standards of the Association for the Advancement of Medical Instrumentation (AAMI) [20], where the maximum acceptable error is 5 ± 8 mmHg. The comparison of our results to the BHS protocol [20] is summarized in Table II. Both SBP and DBP rank grade A.

TABLE II

BP ESTIMATION ACCURACY OF THE BEST PERFORMING MODEL (MODIFIED LENET-5) COMPARED TO THE BHS PROTOCOL. BOTH THE SBP AND THE DBP ESTIMATION ACCURACY RANK GRADE A.

Item	**Percentage** ≤ 5 *mmHg*	≤ 10 *mmHg*	≤ 15 *mmHg*
SBP	69.17%	88.94%	95.05%
DBP	87.85%	97.12%	98.86%
Grade A	60%	85%	95%
Grade B	50%	75%	90%
Grade C	40%	65%	85%

We summarized 5 other recent data-driven works that used PPG signal alone for BP estimation in Table III to compare with our best results produced from the modified LeNet-5 model. As can be seen, our model produces competitive SBP and DBP estimation accuracy, while offering notable simplicity in terms of being free of manual feature engineering, using an ordinary image classification network architecture, and estimating BP with beat-to-beat PPG segments.

TABLE III

PERFORMANCE COMPARISON OF SBP AND DBP ESTIMATION FROM THE PROPOSED METHOD AND RECENT WORKS. ALL LISTED METHODS USED ONLY PPG FOR BP ESTIMATION. N/A IMPLIES "NOT AVAILABLE".

Citation	SBP		DBP	
	ME±SD (mmHg)	MAE (mmHg)	ME±SD (mmHg)	MAE (mmHg)
This work	0.184 ± 7.457	4.673	0.343 ± 4.065	2.476
[21] El Hajj and Kyriacou (2020)	N/A±4.74	3.23	N/A±1.96	1.59
[4] Schlesinger et al. (2020)	N/A±8.65	7.34	N/A±4.48	3.91
[3] Slapničar et al. (2019)	N/A	9.43	N/A	6.88
[22] Xing et al. (2019)	0.45 ± 11.3	N/A	0.31 ± 8.55	N/A
[23] Mousavi et al. (2019)	-0.050 ± 8.901	3.97	0.187 ± 4.173	2.43

IV. CONCLUSIONS

In this study, we presented a method for cuff-less BP monitoring by utilizing VGs created from short PPG segments and a modified LeNet-5 CNN. Our end-to-end method is free of manual feature engineering, requires only PPG signal as input, and can be easily implemented. The model offers standard-compatible BP estimation accuracy while requiring only short, beat-to-beat PPG as its input. As such, the proposed model is a competitive candidate for cuff-less and continuous BP monitoring.

REFERENCES

[1] G. Martínez, N. Howard, D. Abbott, K. Lim, R. Ward, and M. Elgendi, "Can photoplethysmography replace arterial blood pressure in the assessment of blood pressure?" *Journal of Clinical Medicine*, vol. 7, no. 10, p. 316, 2018.

[2] X. Xing and M. Sun, "Optical blood pressure estimation with photoplethysmography and FFT-based neural networks," *Biomedical Optics Express*, vol. 7, no. 8, pp. 3007–3020, 2016.

[3] G. Slapničar, N. Mlakar, and M. Luštrek, "Blood pressure estimation from photoplethysmogram using a spectro-temporal deep neural network," *Sensors*, vol. 19, no. 15, p. 3420, 2019.

[4] O. Schlesinger, N. Vigderhouse, D. Eytan, and Y. Moshe, "Blood pressure estimation from PPG signals using convolutional neural networks and siamese network," in *IEEE International Conference on Acoustics, Speech and Signal Processing (ICASSP)*, 2020, pp. 1135–1139.

[5] A. Krizhevsky, I. Sutskever, and G. E. Hinton, "Imagenet classification with deep convolutional neural networks," *Advances in Neural Information Processing Systems*, vol. 25, pp. 1097–1105, 2012.

[6] Z. Wang and T. Oates, "Imaging time-series to improve classification and imputation," *arXiv preprint arXiv:1506.00327*, 2015.

[7] A. Vilamala, K. H. Madsen, and L. K. Hansen, "Deep convolutional neural networks for interpretable analysis of EEG sleep stage scoring," in *IEEE 27th International Workshop on Machine Learning for Signal Processing (MLSP)*, 2017, pp. 1–6.

[8] K. P. Thanaraj, B. Parvathavarthini, U. J. Tanik, V. Rajinikanth, S. Kadry, and K. Kamalanand, "Implementation of deep neural networks to classify EEG signals using gramian angular summation field for epilepsy diagnosis," *arXiv preprint arXiv:2003.04534*, 2020.

[9] W. Wang, L. Zhu, F. Marefat, P. Mohseni, K. Kilgore, and L. Najafizadeh, "Photoplethysmography-based blood pressure estimation using deep learning," in *to appear in Proc. of 54th Asilomar Conference on Signals, Systems and Computers*. IEEE, 2020.

[10] M. Kachuee, M. M. Kiani, H. Mohammadzade, and M. Shabany, "Cuff-less high-accuracy calibration-free blood pressure estimation using pulse transit time," in *IEEE International Symposium on Circuits and Systems (ISCAS)*, 2015, pp. 1006–1009.

[11] A. L. Goldberger, L. A. Amaral, L. Glass, J. M. Hausdorff, P. C. Ivanov, R. G. Mark, J. E. Mietus, G. B. Moody, C.-K. Peng, and H. E. Stanley, "PhysioBank, PhysioToolkit, and PhysioNet: components of a new research resource for complex physiologic signals," *Circulation*, vol. 101, no. 23, pp. e215–e220, 2000.

[12] [Online]. Available: https://archive.ics.uci.edu/ml/datasets/Cuff-LessBloodPressureEstimation

[13] M. Elgendi, I. Norton, M. Brearley, D. Abbott, and D. Schuurmans, "Systolic peak detection in acceleration photoplethysmograms measured from emergency responders in tropical conditions," *PLOS One*, vol. 8, no. 10, p. e76585, 2013.

[14] L. Lacasa, B. Luque, F. Ballesteros, J. Luque, and J. C. Nuno, "From time series to complex networks: The visibility graph," *Proceedings of the National Academy of Sciences*, vol. 105, no. 13, pp. 4972–4975, 2008.

[15] S. Sannino, S. Stramaglia, L. Lacasa, and D. Marinazzo, "Visibility graphs for fMRI data: multiplex temporal graphs and their modulations across resting state networks," *Network Neuroscience*, 2017.

[16] L. Zhu, C. R. Lee, D. J. Margolis, and L. Najafizadeh, "Decoding cortical brain states from widefield calcium imaging data using visibility graph," *Biomedical Optics Express*, vol. 9, no. 7, pp. 3017–3036, 2018.

[17] L. Zhu, S. Haghani, and L. Najafizadeh, "On fractality of functional near-infrared spectroscopy signals: analysis and applications," *Neurophotonics*, vol. 7, no. 2, p. 025001, 2020.

[18] M. Stephen, C. Gu, and H. Yang, "Visibility graph based time series analysis," *PLOS One*, vol. 10, no. 11, p. e0143015, 2015.

[19] Y. LeCun, L. Bottou, Y. Bengio, and P. Haffner, "Gradient-based learning applied to document recognition," *Proceedings of the IEEE*, vol. 86, no. 11, pp. 2278–2324, 1998.

[20] E. O'brien, B. Waeber, G. Parati, J. Staessen, and M. G. Myers, "Blood pressure measuring devices: recommendations of the European Society of Hypertension," *BMJ*, vol. 322, no. 7285, p. 531, 2001.

[21] C. El Hajj and P. A. Kyriacou, "Cuffless and continuous blood pressure estimation from PPG signals using recurrent neural networks," in *Annual International Conference of The IEEE Engineering in Medicine & Biology Society (EMBC)*, 2020, pp. 4269–4272.

[22] X. Xing, Z. Ma, M. Zhang, Y. Zhou, W. Dong, and M. Song, "An unobtrusive and calibration-free blood pressure estimation method using photoplethysmography and biometrics," *Scientific Reports*, vol. 9, no. 1, p. 8611, 2019.

[23] S. S. Mousavi, M. Firouzmand, M. Charmi, M. Hemmati, M. Moghadam, and Y. Ghorbani, "Blood pressure estimation from appropriate and inappropriate PPG signals using a whole-based method," *Biomedical Signal Processing and Control*, vol. 47, pp. 196–206, 2019.